

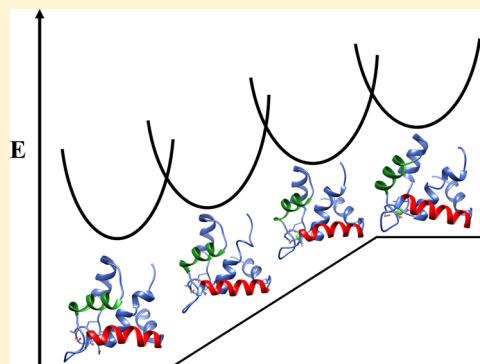
Molecular Dynamics and Umbrella Sampling Simulations Elucidate Differences in Troponin C Isoform and Mutant Hydrophobic Patch Exposure

Jacob D. Bowman and Steffen Lindert*[✉]

Department of Chemistry and Biochemistry, Ohio State University, Columbus, Ohio 43210, United States

Supporting Information

ABSTRACT: Troponin C (TnC) facilitates muscle contraction through calcium-binding within its N-terminal region (NTnC). As previously observed using molecular dynamics (MD) simulations, this calcium-binding event leads to an increase in the dynamics of helices lining a hydrophobic patch on TnC. Simulation times of multiple microseconds were required to even see a partial opening of the hydrophobic patch, limiting the ability to thoroughly and quantitatively investigate these rare events. Here we describe the application of umbrella sampling to probe the TnC hydrophobic patch opening in a more targeted and quantitative fashion. Umbrella sampling was utilized to investigate the differences in the free energy of opening between cardiac (cTnC) and fast skeletal TnC (sTnC). We found that, in agreement with previous reports, holo (calcium-bound) sTnC had a lower free energy of opening compared with holo cTnC. Additionally, differences in the free energy of opening of hypertrophic (HCM) and dilated cardiomyopathy (DCM) cTnC systems were investigated. MD simulations and umbrella sampling revealed a lower free energy of opening for the HCM mutations A8V and A31S, as well as the calcium-sensitizing mutation L48Q. The DCM mutations, Y5H, Q50R, and E59D/D75Y, all exhibited a higher free energy of opening. An umbrella sampling simulation of cTnI-bound holo cTnC exhibited the lowest free energy in the open configuration, in agreement with experimental data. In conclusion, this study presents a novel and successful protocol for applying umbrella sampling simulations to quantitatively study the molecular basis of muscle contraction and proposes a mechanism by which HCM and DCM-associated mutations influence contraction.



INTRODUCTION

Contraction in striated muscle is dictated by sliding of the thin filament against the thick myofibril.¹ Troponin is part of the thin filament and consists of three subunits:² troponin C (calcium-binding subunit), I (inhibitory subunit), and T (tropomyosin-binding subunit). Troponin C, the calcium-binding subunit of troponin, is a two-domain, dumbbell-shaped protein, where each of the two domains contains two EF-hand (helix–loop–helix) motifs.³ The C-terminal domain is referred to as the structural domain and is constitutively bound to calcium or magnesium ions.² The N-terminal domain is referred to as the regulatory domain and is responsible for calcium binding and contraction initiation.⁴ The regulatory domain is also the location of TnI switch peptide-binding. Figure 1A shows the structure of TnC in complex with TnI based on PDB ID 1J1E.⁵ For the regulatory domain to bind the TnI switch peptide, TnC must be in an open conformation, exposing a hydrophobic patch. The degree of hydrophobic patch exposure is described by the interhelical angle between two of its helices (helix A and B).⁶ TnC, in the TnI-bound state, exists in an open conformation with an interhelical angle of approximately 90°, where TnI stabilizes this open conformation of TnC.⁷ In the apo (calcium-free and TnI-free) state of troponin C, these helices are in a closed

conformation with an interhelical angle of approximately 130°. The definitions of the interhelical angle can be seen in Figure S1. In humans, there are two isoforms of TnC that exist in the various muscles of the body: fast skeletal TnC (sTnC) and cardiac/slow skeletal (cTnC).⁹ The structures of cTnC and sTnC are shown in Figure 1B and C, respectively. These isoforms have different calcium binding and structural properties. In sTnC, the N-terminal regulatory domain has two functional calcium binding sites. Binding of two calcium ions allows the domain to stabilize the open conformation in the absence of TnI.¹⁰ The open conformation has been shown in experimentally derived structures of sTnC.^{3,10,11} In cTnC, however, one of the calcium binding sites (site I) is mutated and rendered nonfunctional.⁹ Only a single calcium binds to this domain and is insufficient to stabilize an open conformation.⁴ Previous computational work, however, has shown that the single calcium binding to site II is sufficient to alter the dynamic properties of the cTnC regulatory domain, causing the A and B helices to sample semiopen conformations (interhelical angles less than 110°).⁸ This increased conforma-

Received: June 6, 2018

Revised: July 18, 2018

Published: August 2, 2018

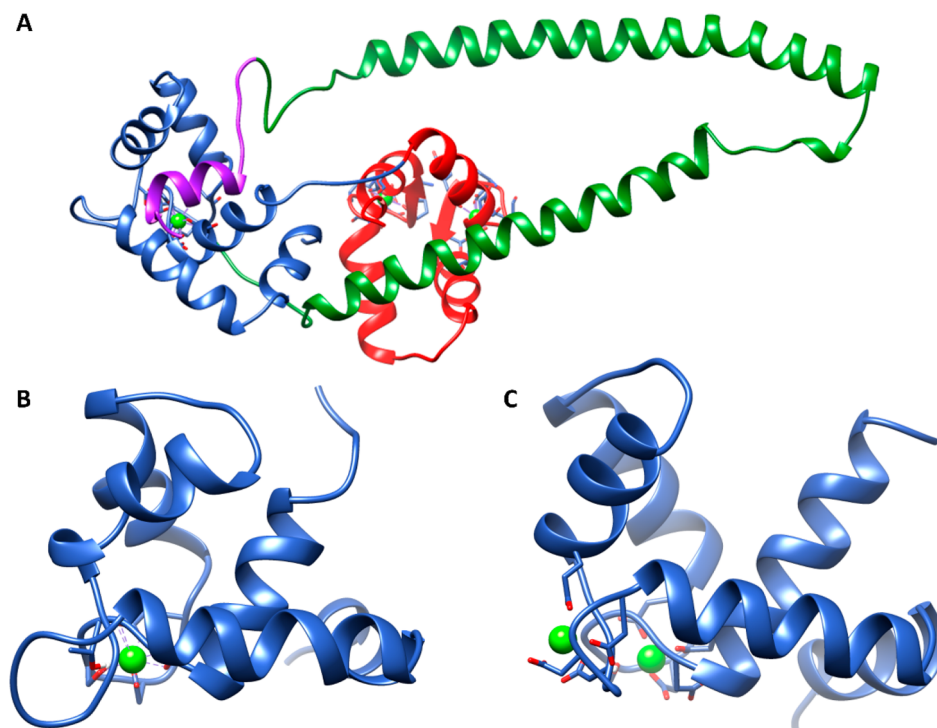


Figure 1. Structures of troponin. (A) Structure of cardiac troponin C in complex with cardiac troponin I. Missing loops have been rebuilt into PDB ID 1J1E. The N-terminal domain of cTnC is highlighted in blue and the TnI-switch peptide is shown in purple. The C-terminal, structural, domain of cTnC is shown in red, and the majority of cTnI is shown in green. The calcium ion is shown as a green sphere. (B) Structure of holo cTnTnC from 1AP4, shown with a single calcium ion bound. The structure is in a closed state with an interhelical angle of 130°. (C) Structure of holo sTnTnC, generated from homology modeling, shown with two calcium ions bound. The structure is in an open state with an interhelical angle of 107°.

tional flexibility has been suggested to support the ability of cTnC to bind the cardiac troponin I (cTnI) switch peptide, and once bound, for cTnI to stabilize the open conformation of cTnC. A molecular level understanding of how the sequences of both these isoforms dictate their dynamic behavior is important to understanding their role in TnC function.

Troponin C sequence alterations introduced by disease mutations are also affecting its dynamics and function. In addition to elucidating the differences between sTnC and cTnC isoforms, a focus of this study will be elucidating the molecular basis of two cardiomyopathies, dilated cardiomyopathy and hypertrophic cardiomyopathy. Dilated cardiomyopathy (DCM) refers to enlargement of the ventricles of the heart and is commonly associated with reduced systole function.¹² DCM has an estimated prevalence of 1 in 2500–3000 people¹³ and an incidence of about 5–8 in 100 000.¹⁴ Hypertrophic cardiomyopathy (HCM) refers to a thickening of the heart muscle tissue and can result in ischemia and diastolic dysfunction.¹⁵ HCM has a prevalence of about 1 in 500, which makes it the most common genetic cardiovascular disease.¹⁵ Mutations in sarcomeric proteins involved in contraction account for approximately 25 to 30% of cases of DCM,¹⁶ and these proteins include actin, myosin, tropomyosin, and all three subunits of troponin.¹⁷ Modifying properties such as cTnC calcium sensitivity, may be a direct cause of these cardiomyopathies. There are several known DCM-associated mutations in the cTnC N-terminal domain that have previously been characterized: Y5H, Q50R, and D75Y/E59D. Y5H, a mutation located in the N-helix of cTnC, showed a lowered calcium sensitivity and altered helical structure

compared to wild-type (WT).^{18,19} Q50R has shown an increase in calcium binding affinity, with a K_d value about a third of that of WT.²⁰ The D75Y/E59D double mutant exhibited a decreased calcium sensitivity in both the C-terminal and N-terminal domain.²¹ There are also several known HCM-associated mutations of cTnC. The mutations studied are all localized in the N-terminal regulatory domain: A8V, L29Q, A31S, and C84Y.^{20,22} A8V, another mutation within the N-helix of cTnC, has been shown to adopt a more open configuration in the apo state and a decreased calcium binding affinity in isolation, but an increased calcium binding affinity in reconstituted thin filament.^{23–25} L29Q has shown a small decrease in calcium sensitivity and was structurally comparable to WT.^{26,27} A31S was also structurally similar to WT and had an increased calcium binding affinity.²⁸ C84Y was structurally different to WT in the apo state and showed no significant change in calcium binding affinity.²⁴ In addition to these known DCM- and HCM-causing mutations, two gain-of-function mutants, L48Q^{29–31} V44Q,^{17,32} and one loss-of-function mutant, E40A,¹⁷ have been studied. In summary, this work, focusing on point mutations of cTnC, showed that the mutations associated with hypertrophic cardiomyopathy (HCM) generally showed an increase in sensitivity to calcium, while dilated cardiomyopathy (DCM) associated mutations showed a decrease in sensitivity to calcium.²²

In addition to the experimental work on troponin C, there have been a growing number of computational studies of cTnC and sTnC in recent years. Due to its relatively small size and importance in heart muscle contraction, cTnC has been studied intensively using molecular dynamics simulations, free energy methods, and docking simulations, where computa-

tional results have frequently been compared to experimental data.^{33–38} One particular focus of computational methods has been the exploration of the hydrophobic patch opening which is difficult to directly measure through experimental methods.^{34,38} cTnC has been shown to have an increased frequency of opening when calcium-bound compared to calcium-free cTnC, whereas gain-of-function and loss-of-function cTnC mutants exhibited altered opening frequencies.⁸ Additionally, properties such as calcium-binding and TnI-switch peptide binding have also been studied extensively. For example, Jayasundar et al. used FRET restraints in molecular dynamics simulations to simulate cTnI interacting with the N-terminal region of cTnC.³⁴ Calcium-binding and TnI-switch peptide binding have been assessed through umbrella sampling,^{20,39} steered molecular dynamics,⁴⁰ and MM/GBSA.^{20,37} The energetics of cTnC calcium-binding has also been assessed through molecular dynamics simulations, where it was shown that calcium binding is less enthalpically favored and more entropically favored in the isolated N-terminal cTnC compared to full-length cTnC.³⁵ In addition to wild-type cTnC, sTnC has also been studied with molecular dynamics to determine a frequency of opening measured by an interhelical distance.⁴¹ cTnC/cTnI binding in HCM/DCM-associated mutations has been investigated directly, in addition to WT cTnC.^{37,42} The molecular effects of cTnC DCM mutations on both calcium sensitivity and myofilament activation have also been investigated.^{20,43,44} Excellent work from Stevens et al. has shown that calcium sensitizing mutations impact the opening frequency of cTnC.²⁰ Up to 1 μ s simulations were performed on HCM-associated (A8V, L29Q, A31S, and C84Y), DCM-associated (Q50R), and calcium-sensitizing (L48Q) mutations. The simulations of L48Q and A31S showed a lower average interhelical angle and a greater distribution of interhelical angles compared to WT.²⁰ L29Q exhibited a lower frequency of opening compared to WT. Additionally, computational studies have contributed to the development of small molecule calcium sensitizing agents.^{45–47} Computational work has also been applied to the whole troponin complex to understand the interactions of the three subunits^{34,48–50} and even part of the thin filament.⁴⁰ One particular focus has been dynamical and functional effects of mutations and PKA phosphorylation of cTnI.^{44,51–56} Finally, models have been developed to describe contraction within the sarcomere.^{48,57–59}

In this work, we used computational techniques to study the dynamic behavior of the cTnC/sTnC isoforms, as well as, known HCM/DCM-causing mutations. Our hypothesis was that the sequence-function relationships of the sTnC/cTnC isoforms and cardiomyopathy mutations are manifested, at least to a significant part, through the different dynamics of TnC hydrophobic patch opening. We hypothesized that HCM-associated mutations will sensitize cTnC, leading to an increased frequency of hydrophobic patch opening and thus a lower free energy of opening. Conversely, we hypothesized that DCM-associated mutations will desensitize cTnC, leading to a decreased frequency of opening and thus a higher free energy of opening compared to WT cTnC. In addition to using well established molecular dynamics (MD) techniques, we have developed an umbrella sampling protocol to probe the free energy landscape of hydrophobic patch opening in a targeted fashion. Compared to MD simulations, the umbrella sampling protocol constituted a significant improvement at consistent and reproducible sampling of hydrophobic patch opening. In MD simulations, we have seen that sTnC isoforms sample

open conformations far more frequently than the cTnC isoform, but not exclusively. The umbrella sampling protocol quantitatively confirmed that sTnC has a lower free energy of opening compared to cTnC. HCM-associated mutations showed an overall increased opening frequency and lower free energy of opening compared to WT. Umbrella sampling simulations of DCM-associated mutations all exhibited a higher free energy of opening compared to WT. Finally, an umbrella sampling simulation of cTnI-bound holo cTnC exhibited the lowest free energy in the open configuration, in agreement with experimental data. In summary, umbrella sampling allowed us to elucidate, at least in part, the role that sequence differences play in the dynamics of the regulatory domains of cTnC and sTnC and how these may ultimately influence the physiology of the skeletal and heart muscle, and diseased states thereof.

METHODS

Homology Modeling. To use molecular dynamics on the human isoform of sTnC, models of the protein were generated using homology modeling. The sequence of the human sTnC protein was extracted from the ENSEMBL⁶⁰ database. Multiple sequence alignments were performed with ClustalOmega.⁶¹ The sequence alignments were utilized for multi-template Rosetta Comparative Modeling (RosettaCM).⁶² The calcium-free form of human sTnC was modeled utilizing chicken calcium-free sTnC (1TNP)³ and turkey calcium-free sTnC (1TRF)¹¹ as the model templates. The calcium-bound form of human sTnC was modeled utilizing rabbit calcium-bound sTnC (1TCF)⁶³ and chicken calcium-bound sTnC (1TNQ).³ RosettaCM accounted for calcium explicitly in modeling of calcium-bound sTnC. 2000 decoys of both calcium-free and calcium-bound sTnC were relaxed in the Rosetta energy function, *talaris2013_cart*.⁶⁴ Rosetta cluster analysis was used to find the lowest energy structure of the largest cluster (with a cluster radius of 2 Å and a limit of 10 clusters). The lowest energy structure was chosen as the starting model for molecular dynamics simulations. The HCM and DCM mutations were introduced with Chimera's⁶⁵ *swapaa* function based on the wild-type calcium-bound cTnC structure 1AP4.⁶⁶

Molecular Dynamics Simulations. System preparation: Eleven different systems of the N-terminal regulatory domains of human troponin C were investigated: wild-type apo sTnC, wild-type holo (Ca²⁺-bound) sTnC, wild-type apo cTnC, wild-type holo cTnC, A8V holo cTnC, A31S holo cTnC, L29Q holo cTnC, L48Q holo cTnC, Y5H holo cTnC, Q50R holo cTnC, and E59D/D75Y holo cTnC. The models used for MD simulations are summarized in Table S1. The initial preparation of the systems is described in detail in⁸ and protonation states were assigned based on an analysis of the starting structures. In short, the systems were solvated with explicit TIP3P water molecules and NaCl counterions were added to neutralize the system and bring it to a final salt concentration of 150 mM. The systems were then restrained, and water molecules were minimized for 10 000 steps. The proteins were then energy minimized for 10 000 steps. The restraints were subsequently removed over 190 000 steps during an equilibration. The final equilibration was 10 000 steps.

Molecular dynamic simulations were carried out using NAMD 2.11⁶⁷ with the CHARMM27 force field⁶⁸ under an NPT ensemble at 310 K with Langevin temperature and

pressure dampening. Bonds with hydrogen were constrained using SHAKE algorithm allowing for a time step of 2 fs. Structures were saved every 2 ps. Production runs were carried out on the Owens Cluster of the Ohio Super Computer (OSC) using 28 processors on 1 node per job, for 500 000 000 timesteps. This corresponded to a total run time of 1 μ s for every system.

Interhelical-Angle Analysis. As previously described in Lindert et al.,⁸ the interhelical angle was calculated utilizing interhlc (K. Yap, University of Toronto, Ontario, Canada). These interhelical angles served as a measure of openness of the TnC hydrophobic patch. Similarly to previous studies,⁸ a Boltzmann distribution of states was used to calculate a relative free energy difference ΔG between the open and closed states: $\Delta G = kT \ln N_{\text{closed}}/N_{\text{open}}$, where k is the Boltzmann constant, T is the temperature of the system, N_{closed} is the number of frames above the closed cutoff (105°), and N_{open} is the number of frames below the closed cutoff.

Umbrella Sampling Protocol. To enhance sampling of the TnC hydrophobic patch opening, we employed umbrella sampling. We used the distance between the N-terminus of helix A and the C-terminus of helix B as the reaction coordinate (“interhelical distance”), describing the transition from closed to open TnC. We defined the interhelical distance as the distance between the three N-terminal backbone atoms (CA, N, C) of helix A (residue 14) and the three C-terminal backbone atoms (CA, N, C) of helix B (residue 48). Umbrella sampling required intermediate conformations along the reaction coordinate to sample the conformational landscape evenly. Because all structures deposited into the PDB existed either in an open (interhelical distances around 28 Å) or closed (interhelical distances around 15 Å) conformation and not in intermediate conformations (interhelical distances between 17 and 25 Å), some starting structures for the umbrella sampling analysis had to be generated via computational methods. To generate starting structures for umbrella sampling, steered molecular dynamics was performed on apo and holo sTnC and cTnC, as well as the HCM/DCM mutations and a cTnI-bound holo cTnC structure (1MXL). The steered MD simulations were performed to open the closed structures of holo cTnC, apo cTnC, apo sTnC, and the HCM/DCM cTnC mutations and to close holo sTnC and cTnI-bound holo cTnC. A constant force of 20 kcal/mol·Å² was applied to the backbone atoms of helices A (residues 14–18; atoms C, CA, N) and B (residues 45–48; atoms C, CA, N) over 5,000,000 steps. These frames were then extracted from the trajectory and an interhelical angle and interhelical distance were calculated from each frame. Umbrella sampling was performed with NAMD using the collective variables to restrain the simulations.^{69,70} During the umbrella sampling run, the interhelical angle could no longer be used as an “on-the-fly” calculation for NAMD. The interhelical distance was thus chosen as the collective variable (colvars). The interhelical distance for the frames in the steered MD trajectory was calculated between the center of mass of the backbone atoms of residues 14 and 48. Representative frames from the steered MD were then selected as windows for the umbrella sampling based on their correlation to the interhelical angle along the transition of closed to open TnC. The path of open to closed interhelical angle was executed from 90° to 140° with 2.5° intervals, which corresponded to approximately a 13 Å interhelical distance range (interhelical distances from 15 to 27 Å, with an ~ 0.5 Å distance interval). Each of the 21

windows was run for 10 ns with a force constant of 50 kcal/mol·Å². Triplicate simulations were run at 310 K under NPT conditions, similar to the microsecond MD simulations. The umbrella sampling simulations were subsequently analyzed via the weighted histogram analysis method.⁷¹ For the WHAM parameters, the max and min values were dictated by the interhelical distance associated with 90° and 140° , respectively. The histogram analysis was divided into 40 bins between the max and min and had a convergence tolerance of 10^{-7} . This analysis generated a free energy profile of the reaction coordinate of opening. The WHAM results from the triplicate simulations were subsequently averaged. The data was linearized with the linear fit function of Matplotlib.⁷²

RESULTS AND DISCUSSION

Longtime MD Simulations and Umbrella Sampling Show Dramatic Opening Frequency Increase of Holo sTnC Compared to Holo cTnC. To analyze and compare the free energy landscape of skeletal and cardiac troponin C, the closed to open hydrophobic patch transition of TnC was assessed by molecular dynamics and umbrella sampling simulations. The opening frequency of calcium-free (apo) and calcium-bound (holo) cTnC and sTnC was first measured by microsecond MD simulations. Apo and holo sTnC and cTnC structures were used as the starting structures for 1 μ s molecular dynamics simulations. As shown in Figure 2A, holo sTnC sampled the open conformation more frequently than holo cTnC. 5.96% and 0.48% of holo sTnC frames were in the semiopen (interhelical angle $\leq 110^\circ$) and open (interhelical angle $\leq 90^\circ$) conformations, respectively. In contrast, only 0.0088% and 0% of holo cTnC frames were in the semiopen and open conformations. Figure 2B shows the distribution of interhelical angles of all four simulated systems. Over the course of the simulation, holo sTnC exhibited a significantly wider distribution of interhelical angles compared to apo sTnC, apo cTnC, and holo cTnC. This finding supported previous experimental data that demonstrated that binding of the two calcium ions is sufficient for opening the hydrophobic patch in sTnC.³ The distributions of interhelical angles of apo cTnC and holo cTnC were not significantly different. We would have expected to see sampling of the open configuration more frequently in the holo cTnC compared to the apo cTnC system. Based on previous simulations⁸ we speculate that seeing these rare opening events in holo cTnC requires simulation times of at least 10 μ s. In complete agreement with experimental observations, the apo isoforms of TnC showed no sampling of the open configuration^{3,4} (Figure 2B). Again, this agreed with previous findings that demonstrated calcium is necessary for sampling the open state of TnC.^{4,66} Using a Boltzmann distribution of states, we extrapolated the free energy of opening for the apo and holo states of both TnC isoforms (Figure 2C). In the microsecond simulations, holo sTnC had a free energy of opening of 4.5 kcal/mol which was much lower than apo sTnC: 9.5 kcal/mol. The lower free energy of opening of holo sTnC agreed with structural data that showed that the two calcium ions are sufficient to stabilize the open configuration.³ Our data suggested, however, that holo sTnC is not exclusively in the open configuration, but also sampled the closed state. This was in agreement to what Genchev et al. showed in their 2013 MD study.⁴¹ A similar extrapolation of apo cTnC and holo cTnC yielded free energies of opening of about 11.5 and 11.6 kcal/mol, respectively. This was in disagreement with previously reported

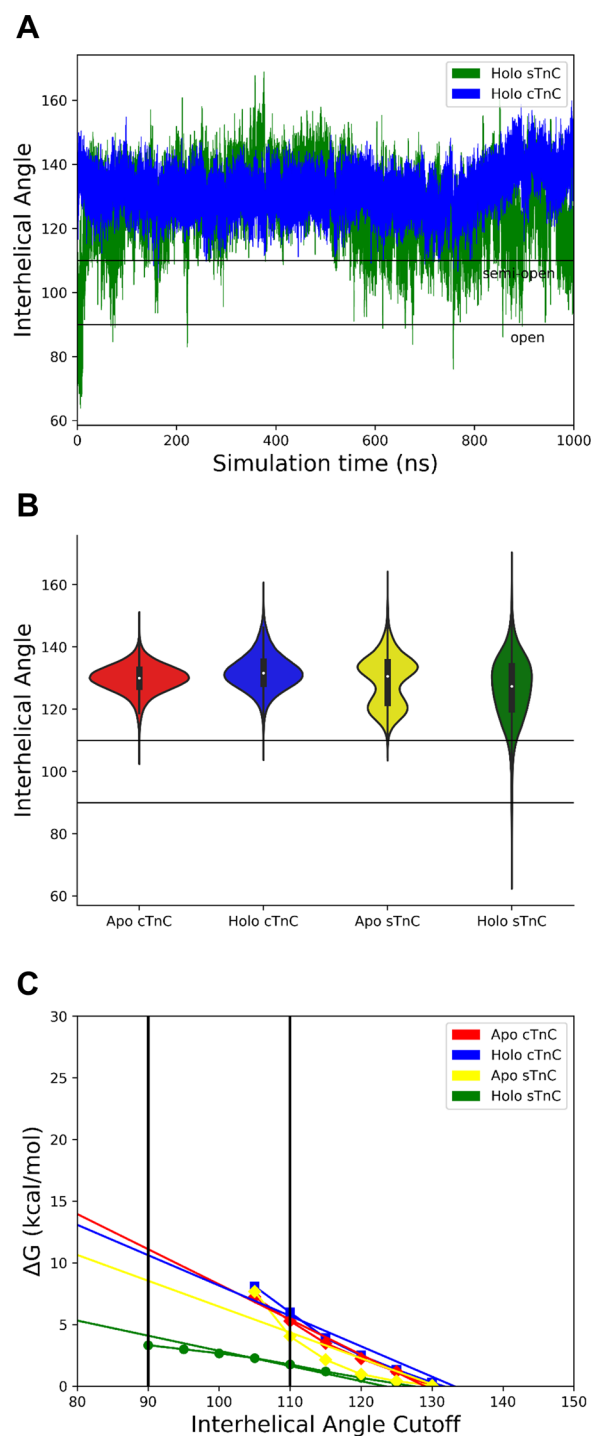


Figure 2. Results of microsecond MD simulations of cTnC and sTnC isoforms. (A) Comparison of interhelical angles of calcium-bound (holo) cTnC (blue) and sTnC (green) over 1 μ s MD simulation time. (B) Distribution of interhelical angles for calcium-free (apo) and holo cTnC and sTnC isoforms over 1 μ s simulation time. We observed a larger distribution, or more sampled opening events, for holo sTnC compared to holo cTnC. (C) Calculated free energy of opening based upon the Boltzmann distribution of states. Holo sTnC showed a lower free energy of opening than holo cTnC, as a result of the holo sTnC system sampling the open state significantly more often than holo cTnC.

longer MD simulations that showed ~ 20 kcal/mol for apo cTnC and ~ 8 kcal/mol for holo cTnC⁸ and with experimental

data suggesting that calcium binding triggers hydrophobic patch opening.^{6,73} This discrepancy was most likely due to the time limitation of the MD simulation and consequently insufficient sampling of the free energy landscape. These results demonstrated the need for a more quantitative evaluation of TnC hydrophobic patch opening using free energy methods.

To offset the limitations of unbiased molecular dynamics simulations and the computational cost of sampling for several microseconds, free energy methods were employed to explore the free energy landscape of troponin hydrophobic patch opening in a more directed fashion. To do this, an umbrella sampling protocol was developed to sample the closed to open transition of apo and holo TnC isoforms. Steered molecular dynamics was used to generate the starting structures for the umbrella sampling windows. Apo sTnC, apo cTnC, and holo cTnC were steered from a closed to an open configuration over 10 ns, while holo sTnC was steered from an open to a closed configuration over 10 ns. Frames from these simulations were extracted and an interhelical angle and distance were calculated. To ensure that the interhelical distance was a suitable proxy for the interhelical angle, the extracted angles and distances were plotted against one another. There was a strong correlation between the angles and distance as seen in Figure S2A. Starting structures were then chosen based on their interhelical angle from 90° to 140° in 2.5° increments and their correlated interhelical distance (from about 12 to 27 Å in ~ 0.5 Å increments). These 21 windows were subsequently utilized in umbrella sampling simulations using the interhelical distance as collective variable. The umbrella sampling simulations, similarly to the steered MD, exhibited complete coverage of all interhelical distances between 12 and 27 Å. Due to the strong correlation between interhelical distances and angles, this also resulted in a complete coverage of interhelical angles between 60° and 150° within the simulations, as seen in Figure S2B. These simulations were analyzed via a weighted histogram analysis method (WHAM) to generate a free energy profile of the hydrophobic patch opening. The results from the umbrella sampling are shown in Figure 3 and summarized in Table 1. The actual free energy profile is shown in Figure S3. We noticed a linear relationship between the free energy and interhelical angle, so the data has been linearized and averaged in Figure S3A. Nonlinearized data is shown in Figure S3B. Our umbrella sampling simulations suggested that the free energy of opening for sTnC holo was 3.0 ± 1.3 kcal/mol which was lower than that of apo sTnC at 9.6 ± 3.2 kcal/mol. These results suggest that holo sTnC can frequently interconvert between open and closed conformations at physiological temperatures. Apo cTnC had a free of opening of 17.5 ± 0.8 kcal/mol which was significantly higher than the holo cTnC, 13.8 ± 2.2 kcal/mol. This agreed with our previous MD simulations⁸ and published experimental data. In summary, the employed umbrella sampling methodology provided a strong alternative to analyze the free energy landscape of TnC hydrophobic patch opening due to the reduced computational cost of using this method and obtaining a more consistent profile compared to the MD simulations. For a comparison of the computational cost, microsecond simulations took about 200 h per system on the Ohio Supercomputer Center utilizing NAMD on 28 CPUs with GPU-acceleration and translated to about 5600 core hours. Umbrella sampling, on the other hand, took on average about 6 h and had an associated cost of 1320

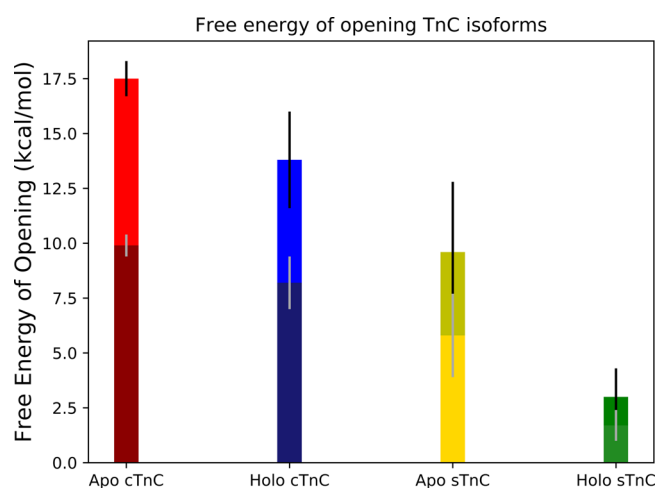


Figure 3. Umbrella sampling results of calcium-free (apo) and calcium-bound (holo) cTnC/sTnC isoforms. The darker shades are the free energies to open the systems to an interhelical angle of 110° (i.e., a semiopen conformation), and the lighter shades are the free energies to open the systems to an interhelical angle of 90° (i.e., a fully open conformation). Free energies of opening were determined by WHAM analysis of umbrella sampling simulations. Apo forms of TnC exhibited a higher free energy of opening compared to the corresponding holo isoform. sTnC exhibited a lower free energy of opening compared to the cTnC isoform. sTnC holo had a significantly lower free energy of opening compared to cTnC holo.

Table 1. Free Energy of Opening, As Determined by WHAM Analysis of Umbrella Sampling Simulations, for Each TnC Isoform, HCM-Associated, and DCM-Associated Mutations

TnC isoform	free energy of opening(kcal/mol)
Apo cTnC	17.5 ± 0.8
Holo cTnC	13.8 ± 2.2
Apo sTnC	9.6 ± 3.2
Holo sTnC	3.0 ± 1.3
TnI-bound Holo cTnC	-6.3 ± 0.2
HCM mutant	
A8V	11.1 ± 0.8
L29Q	12.2 ± 2.2
A31S	10.1 ± 2.4
L48Q	8.3 ± 0.5
DCM mutant	
Y5H	18.7 ± 1.9
Q50R	17.0 ± 1.1
E59D/D75Y	22.7 ± 5.7

core hours, which was about a 4-fold reduction in computational cost and a 33-fold reduction in run time.

Longtime MD Simulations and Umbrella Sampling of HCM-Associated and Calcium-Sensitizing cTnC Mutations Exhibit an Increase in Opening Events. To investigate the molecular role that HCM-associated and calcium-sensitizing cTnC mutations play in the physiology of the heart, the impact of these mutations on the dynamics of cTnC was studied, with a particular focus on differences in hydrophobic patch opening. We investigated three HCM mutations (A8V, L29Q, A31S) and one calcium-sensitizing mutation (L48Q) and performed 1 μ s MD simulations for each cTnC system in the calcium-bound state. Figure S4 shows the locations of these mutations on cTnC. Figure 4A shows

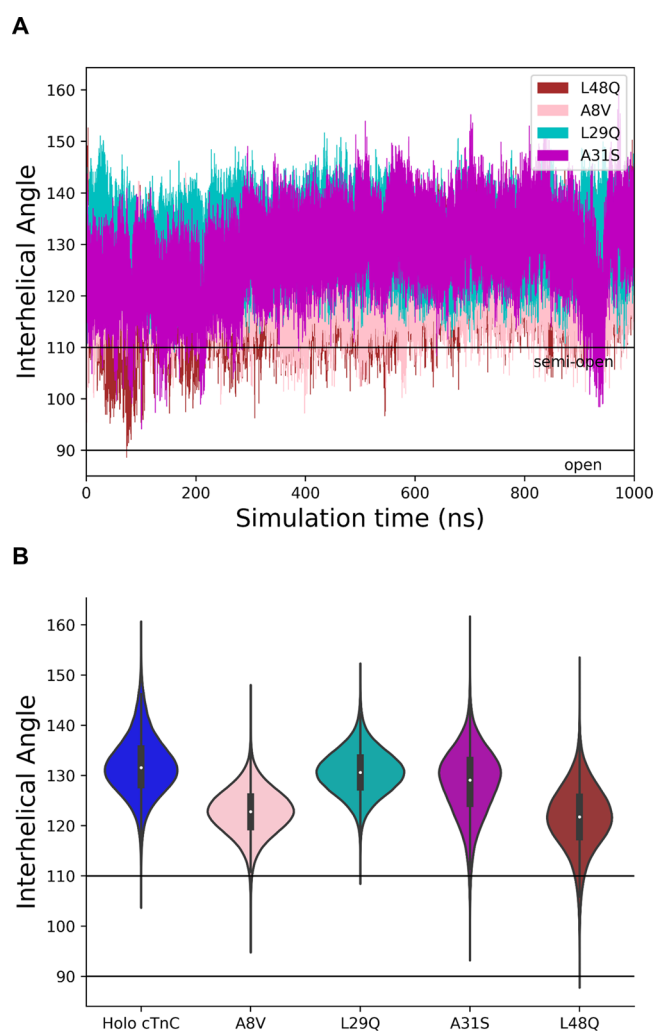


Figure 4. Results of microsecond MD simulations of holo cTnC HCM mutants. (A) Interhelical angles of HCM mutants and L48Q during 1 μ s MD simulations. L48Q sampled the open configuration more often than the HCM-associated mutations. The HCM mutations did not sample fully open configurations, but rather frequently semiopen configurations. (B) Distribution of interhelical angles of HCM-associated mutations and L48Q. L48Q showed sampling of the semiopen and open states more often than the HCM-associated mutations and WT.

the interhelical angle between cTnC helices A and B as a function of simulation time for all four microsecond simulations, while Figure 4B shows the distribution of interhelical angles of all four simulated systems and WT as violin plots. L48Q exhibited a significant increase in the number of opening events compared to WT during the microsecond simulation. 4.37% of L48Q cTnC frames were in the semiopen (interhelical angle $\leq 110^\circ$) conformation, compared to only 0.0088% of wild-type cTnC frames. The HCM-associated mutations, in general, sampled the semiopen configuration more often than the WT. On average 0.52% of frames corresponding to the HCM-associated mutant systems were in the semiopen conformation. L29Q sampled the open configuration similarly to the WT cTnC (0.002% of frames in the semiopen conformation). As observed for the WT skeletal and cardiac systems, this might suggest the lack of sufficient sampling to show a discernible difference in the opening frequency or WT and L29Q. Using a Boltzmann distribution of

states based on the simulation results, the free energy of opening for all systems was estimated as a function of the interhelical angle from the MD simulations (Figure S5). However, due to limited sampling, the consequences of the HCM associated mutations on the relative free energy of opening could not be reliably deduced from the MD simulations. To conduct a more exhaustive search of the free energy landscape, umbrella sampling simulations were performed on the HCM mutations (A8V, L29Q, A31S) and the calcium sensitizing mutation L48Q, followed by a WHAM analysis to generate a free energy profile of the hydrophobic patch opening. A summary of these results can be seen in Figure 5 and Table 1. Complete, nonlinearized and linearized

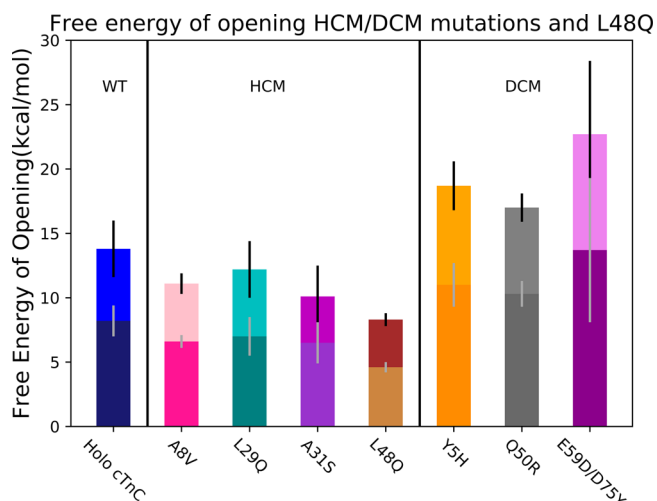


Figure 5. Umbrella sampling results of calcium-bound (holo) HCM-associated and calcium-sensitizing mutations, as well as DCM-associated mutations compared to wild-type holo cTnC (blue). The darker shades are the free energies to open the systems to an interhelical angle of 110° (i.e., a semiopen conformation), and the lighter shades are the free energies to open the systems to an interhelical angle of 90° (i.e., a fully open conformation). Free energies of opening were determined by WHAM analysis of umbrella sampling simulations. HCM-associated mutations all exhibited a lower free energy of opening compared to WT and L48Q showed the lowest free energy of opening. DCM-associated mutations all exhibited a higher free energy of opening compared to WT holo cTnC.

data is shown in Figure S6. These simulations showed that the HCM mutations A8V ($\Delta G \sim 11.1$ kcal/mol), A31S ($\Delta G \sim 10.1$ kcal/mol) and the calcium sensitizing mutation L48Q ($\Delta G \sim 8.3$ kcal/mol) had a lower free energy of opening compared to WT holo cTnC. Interestingly, L29Q exhibited a free energy of opening on par with WT holo cTnC (12.2 ± 2.2 kcal/mol and 13.8 ± 2.2 kcal/mol, respectively) as seen in Table 1. This agreed with our MD simulations that showed the distribution of angles for L29Q was similar to WT cTnC, negating our initial hypothesis of limited sampling. We are thus speculating that L29Q impacts other features of cTnC, such as calcium binding or cTnI binding.

Umbrella Sampling of Human DCM-Associated cTnC Mutations Show an Increase in Free Energy of Opening. We also investigated the molecular impact of DCM-associated cTnC mutations on the dynamics of troponin C hydrophobic patch opening. We performed 1 μ s MD simulations for three calcium-bound cTnC DCM mutant systems (Y5H, Q50R, and the double mutant E59D/D75Y).

Figure S7A shows the interhelical angle between cTnC helices A and B as a function of simulation time for all three microsecond simulations, while Figure S7B shows the distribution of interhelical angles of all three simulated systems as violin plots. DCM-associated mutation Q50R exhibited a similar interhelical angle distribution to WT. Y5H opened slightly more frequently than WT. This might suggest the histidine mutation is destabilizing the closed configuration of cTnC in the calcium bound state. D75Y/E59D also sampled the open configuration transiently, however the distribution of the interhelical angles over the microsecond suggested that it spent most of its time in the closed configuration, as seen in Figure S7B. Using a Boltzmann distribution of states based on the simulation results, the free energy of opening for DCM-associated mutations was estimated as a function of the interhelical angle from the MD simulations (Figure S8). While these limited MD simulation results seemed to contradict our initial hypothesis that the sequence-function relationship of DCM mutations was manifested in a decrease in hydrophobic patch opening, we speculated that due to the limited MD sampling, the relative free energy of opening of DCM mutant systems could not be reliably deduced from the MD simulations. Hence, we performed umbrella sampling simulations and a WHAM analysis on the three holo cTnC DCM mutant systems in order to obtain a more accurate representation of the free energy profile of hydrophobic patch opening. Results of the umbrella sampling are shown in Figure 5 and Table 1. Complete, nonlinearized and linearized data is shown in Figure S9. Umbrella sampling was able to more quantitatively discern the effect of these mutations than MD simulations alone. These simulations showed that the DCM mutations Y5H ($\Delta G \sim 18.7$ kcal/mol), Q50R ($\Delta G \sim 17.0$ kcal/mol), and the double mutant E59D/D75Y ($\Delta G \sim 22.7$ kcal/mol) indeed had a higher free energy of hydrophobic patch opening compared to WT holo cTnC. This corroborated our initial hypothesis, that these mutations likely stabilize the closed conformation of holo cTnC, which would lead to an increased free energy cost of opening to overcome that stabilization.

Umbrella Sampling of cTnI-Bound Holo cTnC Confirmed That Open Conformation Is Stable. None of the systems studied so far had the cTnI switch peptide bound. Binding of the switch peptide should stabilize the open configuration. To investigate the ability of umbrella sampling to accurately describe the free energy profile, cTnI-bound holo cTnC (1MXL)⁶ was simulated. This starting structure was in the open configuration and was closed in the steered MD simulation with cTnI present within the hydrophobic patch. The resulting, averaged and linearized WHAM analysis free energy profile can be seen in Figure 6. The raw data is shown in Figure S10. The lowest free energy now was in the open conformation, at around -6.3 kcal/mol. This value is a relative free energy of opening calculated from the difference between the energy levels of the closed and open conformations. As seen in Figure S11, the closing of the cTnI-bound holo cTnC during the umbrella sampling caused an unraveling of the switch peptide to accommodate the closing. This demonstrates the ability of umbrella sampling to discern the lowest energy state of a wide variety of cTnC systems.

CONCLUSIONS

We performed microsecond MD simulations and developed an umbrella sampling protocol to investigate the free energy

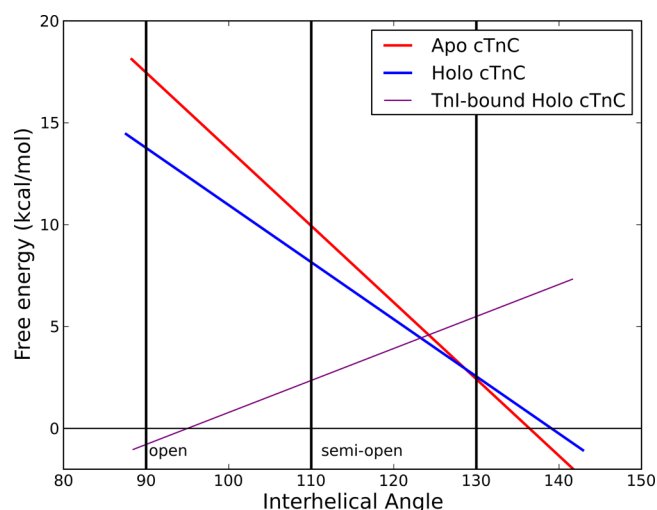


Figure 6. WHAM analysis results of umbrella sampling of apo cTnC, holo cTnC, and TnI-bound holo cTnC. TnI-bound holo cTnC exhibited its most stable conformation in the open configuration due to stabilization from the TnI switch peptide.

landscape of TnC hydrophobic patch opening. Microsecond MD simulations exhibited large differences between the sTnC and cTnC isoforms, as well as, more pronounced interhelical angle distributions for HCM mutations. However, generally, we were unable to extract more subtle differences between the isoforms and mutants from the microsecond MD simulations as a direct consequence of the unbiased nature of the simulations and a resulting insufficient sampling of the hydrophobic patch opening. The umbrella sampling protocol developed here allowed for a more direct and targeted sampling of the free energy landscape, obviating the need for the MD simulations to randomly sample an open configuration. Not only did this method improve the sampling but provided a significantly reduced computational cost to quantitatively study TnC hydrophobic patch opening.

MD and umbrella sampling simulations of the holo sTnC isoform suggested a dramatic increase in open configurations compared to the holo cTnC isoform, however the simulations also indicated that the system spends the majority of the time in an at least semiclosed state. This is in agreement with previous MD studies on sTnC where the open structure closed during the simulation. Potentially, the presence of calcium in site I is sufficient to open the system on longer time scales inaccessible by simulation methods but accessible by structure determination methods. Future work is advised to reconcile computational and experimental observations. As hypothesized, HCM and calcium-sensitizing mutations, on average, showed a lower free energy of opening compared to the WT cTnC. This can be explained by the substitution of hydrophobic amino acids with charged or more hydrophilic amino acids within the hydrophobic patch area and a subsequent destabilization of hydrophobic packing. The fact that these mutations altered the free energy to varying degrees suggests that the mechanism of hydrophobic patch opening could be modulated for a specific response. Likewise, DCM and calcium-desensitizing mutations increased the free energy of opening to varying degrees. Finally, cTnI-bound holo cTnC exhibited the lowest free energy in the open configuration, in agreement with experimental data. Probing specific interactions through the computational methods discussed has

shown to be critical in understanding muscle contraction at a molecular level.

To summarize, we showed that the free energy of TnC opening can be more effectively probed by umbrella sampling in comparison to traditional MD simulations. This methodology significantly reduced the required computational resources and time to understand the role mutations play in the function of TnC. Umbrella sampling has been previously applied to TnC calcium-binding free energy, but, to our knowledge, this is the first use of it to study the free energy of hydrophobic patch opening. This is an encouraging development for studying TnC, understanding the molecular processes involved in muscle contraction and developing more specific treatments for its associated diseases.

■ ASSOCIATED CONTENT

Supporting Information

The Supporting Information is available free of charge on the ACS Publications website at DOI: 10.1021/acs.jpcc.8b05435.

Definition of the interhelical angle; correlation data between interhelical angle and interhelical distances; raw and linearized umbrella sampling data of cTnC, sTnC, HCM, DCM, and TnI-bound cTnC; locations of HCM and DCM mutations in cTnC regulatory domain; calculated free energy of opening from microsecond MD simulations of HCM and DCM; interhelical angle distributions of DCM; starting frames of cTnI-bound cTnC umbrella sampling (PDF)

■ AUTHOR INFORMATION

Corresponding Author

*Mailing address: Department of Chemistry and Biochemistry, Ohio State University 2114 Newman & Wolfrom Laboratory, 100 W. 18th Avenue, Columbus, OH 43210. Phone: 614-292-8284. Fax: 614-292-1685. E-mail: lindert.1@osu.edu.

ORCID

Steffen Lindert: 0000-0002-3976-3473

Notes

The authors declare no competing financial interest.

■ ACKNOWLEDGMENTS

The authors would like to thank Jeff Wereszczynski for advice on umbrella sampling simulations. We thank the members of the Lindert lab for many useful discussions. We would like to thank the Ohio Supercomputer Center for valuable computational resources.⁷⁴ This work was supported by NIH (R01 HL137015) to S.L. Additionally, work in the Lindert laboratory is supported through NIH (R03 AG054904), NSF (CHE 1750666), and a Falk Medical Research Trust Catalyst Award.

■ REFERENCES

- (1) Spudich, J. A.; Watt, S. The Regulation of Rabbit Skeletal Muscle Contraction. *J. Biol. Chem.* **1971**, *246* (15), 4866–4871.
- (2) Li, M. X.; Hwang, P. M. Structure and Function of Cardiac Troponin C (TNNC1): Implications for Heart Failure, Cardiomyopathies, and Troponin Modulating Drugs. *Gene* **2015**, *571* (2), 153–166.
- (3) Sundaralingam, M.; Bergstrom, R.; Strasburg, S.; Rao, S. T.; Roychowdhury, P.; Greaser, M.; Wang, B. C. Molecular Structure of Troponin C from Chicken Skeletal Muscle at 3-Angstrom Resolution. *Science* **1985**, *227* (4689), 945–948.

- (4) Sia, S. K.; Li, M. X.; Gagne, S.; Liu, W.; Putkey, J. A.; Sykes, B. D. Structure of Cardiac Muscle Troponin C Unexpectedly Reveals a Closed Regulatory Domain. *J. Biol. Chem.* **1997**, *272* (29), 18216–18221.
- (5) Takeda, S.; Yamashita, A.; Maeda, K.; Maéda, Y. Structure of the Core Domain of Human Cardiac Troponin in the Ca²⁺-saturated Form. *Nature* **2003**, *424*, 35–41.
- (6) Li, M. X.; Spyropoulos, L.; Sykes, B. D. Binding of Cardiac Troponin-I 147–163 Induces a Structural Opening in Human Cardiac Troponin-C. *Biochemistry* **1999**, *38* (26), 8289–8298.
- (7) Herzberg, O.; Moul, J.; James, M. N. G. A Model for the Ca²⁺-induced Conformational Transition of Troponin C. A Trigger for Muscle Contraction. *J. Biol. Chem.* **1986**, *261* (6), 2638–2644.
- (8) Lindert, S.; Kekenus-Huskey, P. M.; McCammon, J. A. Long-timescale Molecular Dynamics Simulations Elucidate the Dynamics and Kinetics of Exposure of the Hydrophobic Patch in Troponin C. *Biophys. J.* **2012**, *103* (8), 1784–1789.
- (9) Wang, Y.-P.; Fuchs, F. Length, Force, and Ca²⁺-troponin C Affinity in Cardiac and Slow Skeletal Muscle. *Am. J. Physiol.* **1994**, *266*, C1077–C1082.
- (10) Gagne, S. M.; Tsuda, S.; Li, M. X.; Smillie, L. B.; Sykes, B. D. Structures of the Troponin C Regulatory Domains in the Apo and Calcium-saturated States. *Nat. Struct. Mol. Biol.* **1995**, *2* (9), 784–789.
- (11) Findlay, W. A.; Sonnichsen, F. D.; Sykes, B. D. Solution Structure of the TRIC Fragment of Skeletal Muscle. *J. Biol. Chem.* **1994**, *269* (9), 6773–6778.
- (12) McNally, E. M.; Golbus, J. R.; Puckelwartz, M. J. Genetic Mutations and Mechanisms in Dilated Cardiomyopathy. *J. Clin. Invest.* **2013**, *123* (1), 19–26.
- (13) Codd, M. B.; Sugrue, D. D.; Gersh, B. J.; Melton, L. J., III Epidemiology of Idiopathic Dilated and Hypertrophic Cardiomyopathy. *Circulation* **1989**, *80* (3), 564–572.
- (14) Kärkkäinen, S.; Peuhkurinen, K. Genetics of Dilated Cardiomyopathy. *Ann. Med.* **2007**, *39* (2), 91–107.
- (15) Maron, B. J. Hypertrophic Cardiomyopathy: A Systematic Review. *J. Am. Med. Assoc.* **2002**, *287* (10), 1308–1320.
- (16) Kamisago, M.; Sharma, S. D.; DePalma, S. R.; Solomon, S.; Sharma, P.; McDonough, B.; Smoot, L.; Mullen, M. P.; Woolf, P. K.; Wigle, E. D.; et al. Mutations in Sarcomere Protein Genes as a Cause of Dilated Cardiomyopathy. *N. Engl. J. Med.* **2000**, *343* (23), 1688–1696.
- (17) Parvatiyar, M. S.; Pinto, J. R.; Liang, J.; Potter, J. D. Predicting Cardiomyopathic Phenotypes by Altering Ca²⁺ affinity of Cardiac Troponin C. *J. Biol. Chem.* **2010**, *285* (36), 27785–27797.
- (18) Pinto, J. R.; Siegfried, J. D.; Parvatiyar, M. S.; Li, D.; Norton, N.; Jones, M. A.; Liang, J.; Potter, J. D.; Hershberger, R. E. Functional Characterization of TNNC1 Rare Variants Identified in Dilated Cardiomyopathy. *J. Biol. Chem.* **2011**, *286* (39), 34404–34412.
- (19) Hershberger, R. E.; Norton, N.; Morales, A.; Li, D.; Siegfried, J. D.; Gonzalez-Quintana, J. Coding Sequence Rare Variants Identified in MYBPC3, MYH6, TPM1, TNNC1, and TNN13 From 312 Patients With Familial or Idiopathic Dilated Cardiomyopathy. *Circ.: Cardiovasc. Genet.* **2010**, *3*, 155–161.
- (20) Stevens, C. M.; Rayani, K.; Singh, G.; Lotfalismasi, B.; Tieleman, D. P.; Tibbitts, G. F. Changes in the Dynamics of the Cardiac Troponin C Molecule Explain the Effects of Ca²⁺-sensitizing Mutations. *J. Biol. Chem.* **2017**, *292* (28), 11915–11926.
- (21) Dweck, D.; Reynaldo, D. P.; Pinto, J. R.; Potter, J. D. A Dilated Cardiomyopathy Troponin C Mutation Lowers Contractile Force by Reducing Strong Myosin-Actin Binding. *J. Biol. Chem.* **2010**, *285* (23), 17371–17379.
- (22) Kalyva, A.; Parthenakis, F. I.; Marketou, M. E.; Kontarakis, J. E.; Vardas, P. E. Biochemical Characterisation of Troponin C Mutations Causing Hypertrophic and Dilated Cardiomyopathies. *J. Muscle Res. Cell Motil.* **2014**, *35* (2), 161–178.
- (23) Swindle, N.; Tikunova, S. B. Hypertrophic Cardiomyopathy-Linked Mutation D145E Drastically Alters Calcium Binding by the C-Domain of Cardiac Troponin C. *Biochemistry* **2010**, *49*, 4813–4820.
- (24) Pinto, J. R.; Parvatiyar, M. S.; Jones, M. A.; Liang, J.; Ackerman, M. J.; Potter, J. D. A Functional and Structural Study of Troponin C Mutations Related to Hypertrophic Cardiomyopathy. *J. Biol. Chem.* **2009**, *284* (28), 19090–19100.
- (25) Cordina, N. M.; Liew, C. K.; Gell, D. A.; Fajer, P. G.; Mackay, J. P.; Brown, L. J. Effects of Calcium Binding and the Hypertrophic Cardiomyopathy A8V Mutation on the Dynamic Equilibrium between Closed and Open Conformations of the Regulatory N-Domain of Isolated Cardiac Troponin C. *Biochemistry* **2013**, *52*, 1950–1962.
- (26) Gollapudi, S. K.; Chandra, M. Cardiomyopathy-Related Mutations in Cardiac Troponin C, L29Q and G159D, Have Divergent Effects on Rat Cardiac Myofiber Contractile Dynamics. *Biochem. Res. Int.* **2012**, *2012*, 824068.
- (27) Dweck, D.; Hus, N.; Potter, J. D. Are Changes in the Ca²⁺ Sensitivity of Myofilaments Containing Cardiac Troponin C Mutations (G159D and L29Q) Good Predictors of the Phenotypic Outcomes? *J. Biol. Chem.* **2008**, *283* (48), 33119–33128.
- (28) Parvatiyar, M. S.; Landstrom, A. P.; Figueiredo-Freitas, C.; Potter, J. D.; Ackerman, M. J.; Pinto, J. R. A Mutation in TNNC1-encoded Cardiac Troponin C, TNNC1-A31S, Predisposes to Hypertrophic Cardiomyopathy and Ventricular Fibrillation. *J. Biol. Chem.* **2012**, *287* (38), 31845–31855.
- (29) Shettigar, V.; Zhang, B.; Little, S. C.; Salhi, H. E.; Hansen, B. J.; Li, N.; Zhang, J.; Roof, S. R.; Ho, H.-T.; Brunello, L.; et al. Rationally Engineered Troponin C Modulates In Vivo Cardiac Function and Performance in Health and Disease. *Nat. Commun.* **2016**, *7*, 10794.
- (30) Feest, E. R.; Steven Korte, F.; Tu, A.-Y.; Dai, J.; Razumova, M. V.; Murry, C. E.; Regnier, M. Thin Filament Incorporation of an Engineered Cardiac Troponin C Variant (L48Q) Enhances Contractility in Intact Cardiomyocytes from Healthy and Infarcted Hearts. *J. Mol. Cell. Cardiol.* **2014**, *72* (206), 219–227.
- (31) Wang, D.; Robertson, I. M.; Li, M. X.; McCully, M. E.; Crane, M. L.; Luo, Z.; Tu, A.-Y.; Daggett, V.; Sykes, B. D.; Regnier, M. Structural and Functional Consequences of the Cardiac Troponin C L48Q Ca²⁺-sensitizing Mutation. *Biochemistry* **2012**, *51* (22), 4473–4487.
- (32) Tikunova, S. B.; Davis, J. P. Designing Calcium-sensitizing Mutations in the Regulatory Domain of Cardiac Troponin C. *J. Biol. Chem.* **2004**, *279* (34), 35341–35352.
- (33) Papadaki, M.; Marston, S. B. The Importance of Intrinsically Disordered Segments of Cardiac Troponin in Modulating Function by Phosphorylation and Disease-Causing Mutations. *Front. Physiol.* **2016**, *7*, 508.
- (34) Jayasundar, J. J.; Xing, J.; Robinson, J. M.; Cheung, H. C.; Dong, W.-J. Molecular Dynamics Simulations of the Cardiac Troponin Complex Performed with FRET Distances as Restraints. *PLoS One* **2014**, *9* (2), e87135.
- (35) Skowronsky, R. A.; Schroeter, M.; Baxley, T.; Li, Y.; Chalovich, J. M.; Spuches, A. M. Thermodynamics and Molecular Dynamics Simulations of Calcium Binding to the Regulatory Site of Human Cardiac Troponin C: Evidence for Communication with the Structural Calcium Binding Sites. *JBIC, J. Biol. Inorg. Chem.* **2013**, *18*, 49–58.
- (36) Varughese, J. F.; Li, Y. Molecular Dynamics and Docking Studies on Cardiac Troponin C. *J. Biomol. Struct. Dyn.* **2011**, *29* (1), 123–135.
- (37) Lindert, S.; Kekenus-Huskey, P. M.; Huber, G.; Pierce, L.; McCammon, J. A. Dynamics and Calcium Association to the N-terminal Regulatory Domain of Human Cardiac Troponin C: A Multiscale Computational Study. *J. Phys. Chem. B* **2012**, *116* (29), 8449–8459.
- (38) Cordina, N. M.; Liew, C. K.; Potluri, P. R.; Curmi, P. M.; Fajer, P. G.; Logan, T. M.; Mackay, J. P.; Brown, L. J. Ca²⁺-Induced PRE-NMR Changes in the Troponin Complex Reveal the Possessive Nature of the Cardiac Isoform for Its Regulatory Switch. *PLoS One* **2014**, *9* (11), e112976.
- (39) Stevens, C. M.; Rayani, K.; Genge, C. E.; Singh, G.; Liang, B.; Roller, J. M.; Li, C.; Li, A. Y.; Tieleman, D. P.; van Petegem, F.;

Tibbitts, G. F. Characterization of Zebrafish Cardiac and Slow Skeletal Troponin C Paralogs by MD Simulation and ITC. *Biophys. J.* **2016**, *111* (1), 38–49.

(40) Williams, M. R.; Lehman, S. J.; Tardiff, J. C.; Schwartz, S. D. Atomic Resolution Probe for Allostery in the Regulatory Thin Filament. *Proc. Natl. Acad. Sci. U. S. A.* **2016**, *113* (12), 3257–3262.

(41) Genchev, G. Z.; Kobayashi, T.; Lu, H. Calcium Induced Regulation of Skeletal Troponin — Computational Insights from Molecular Dynamics Simulations. *PLoS One* **2013**, *8* (3), e58313.

(42) Wang, D.; McCully, M. E.; Luo, Z.; McMichael, J.; Tu, A.-Y.; Daggett, V.; Regnier, M. Structural and Functional Consequences of Cardiac Troponin C L57Q and I61Q Ca²⁺-desensitizing Variants. *Arch. Biochem. Biophys.* **2013**, *535* (1), 68–75.

(43) Lim, C. C.; Yang, H.; Yang, M.; Wang, C. K.; Shi, J.; Berg, E. A.; Pimentel, D. R.; Gwathmey, J. K.; Hajjar, R. J.; Helmes, M.; et al. A Novel Mutant Cardiac Troponin C Disrupts Molecular Motions Critical for Calcium Binding Affinity and Cardiomyocyte Contractility. *Biophys. J.* **2008**, *94* (9), 3577–3589.

(44) Dewan, S.; McCabe, K. J.; Regnier, M.; McCulloch, A. D.; Lindert, S. Molecular Effects of cTnC DCM Mutations on Calcium Sensitivity and Myofilament Activation - An Integrated Multi-scale Modeling Study. *J. Phys. Chem. B* **2016**, *120* (33), 8264–8275.

(45) Varughese, J. F.; Li, Y. Molecular Dynamics and Docking Studies on Cardiac Troponin C. *J. Biomol. Struct. Dyn.* **2011**, *29* (1), 123–135.

(46) Lindert, S.; Li, M. X.; Sykes, B. D.; McCammon, J. A. Computer-aided Drug Discovery Approach Finds Calcium Sensitizer of Cardiac Troponin. *Chem. Biol. Drug Des.* **2015**, *85* (2), 99–106.

(47) Aprahamian, M. L.; Tikunova, S. B.; Price, M. V.; Cuesta, A. F.; Davis, J. P.; Lindert, S. Successful Identification of Cardiac Troponin Calcium Sensitizers Using a Combination of Virtual Screening and ROC Analysis of Known Troponin C Binders. *J. Chem. Inf. Model.* **2017**, *57* (12), 3056–3069.

(48) Manning, E. P.; Tardiff, J. C.; Schwartz, S. D. A Model of Calcium Activation of the Cardiac Thin Filament. *Biochemistry* **2011**, *50* (34), 7405–7413.

(49) Varughese, J. F.; Chalovich, J. M.; Lit, Y. Molecular Dynamics Studies on Troponin (TnI-TnT-TnC) Complexes: Insight into the Regulation of Muscle Contraction. *J. Biomol. Struct. Dyn.* **2010**, *28* (2), 159–174.

(50) Varughese, J. F.; Baxley, T.; Chalovich, J. M.; Li, Y. A Computational and Experimental Approach To Investigate Bepridil Binding with Cardiac Troponin. *J. Phys. Chem. B* **2011**, *115* (10), 2392–2400.

(51) Wabik, J.; Kurcinski, M.; Kolinski, A. Flexible Docking of the Fragment of the Troponin I to the Troponin C. *IWBBIO 2014 (2nd International Work-Conference on Bioinformatics and Biomedical Engineering)*; 2014; pp 1064–1073.

(52) Dvornikov, A. V.; Smolin, N.; Zhang, M.; Martin, J. L.; Robia, S. L.; De Tombe, P. P. Restrictive Cardiomyopathy Troponin I R145W Mutation Does Not Perturb Myofilament Length-dependent Activation in Human Cardiac Sarcomeres. *J. Biol. Chem.* **2016**, *291* (41), 21817–21828.

(53) Cheng, Y.; Lindert, S.; Kekenus-Huskey, P.; Rao, V. S.; Solaro, R. J.; Rosevear, P. R.; Amaro, R.; McCulloch, A. D.; McCammon, J. A.; Regnier, M. Computational Studies of the Effect of the S23D/S24D Troponin I Mutation on Cardiac Troponin Structural Dynamics. *Biophys. J.* **2014**, *107* (7), 1675–1685.

(54) Cheng, Y.; Rao, V.; Tu, A.-Y.; Lindert, S.; Wang, D.; Oxenford, L.; McCulloch, A. D.; McCammon, J. A.; Regnier, M. Troponin I Mutations R146G and R21C Alter Cardiac Troponin Function, Contractile Properties, and Modulation by Protein Kinase A (PKA)-mediated Phosphorylation. *J. Biol. Chem.* **2015**, *290* (46), 27749–27766.

(55) Cheng, Y.; Lindert, S.; Oxenford, L.; Tu, A.-Y.; McCulloch, A. D.; Regnier, M. Effects of Cardiac Troponin I Mutation P83S on Contractile Properties and the Modulation by PKA-Mediated Phosphorylation. *J. Phys. Chem. B* **2016**, *120* (33), 8238–8253.

(56) Lindert, S.; Cheng, Y.; Kekenus-Huskey, P.; Regnier, M.; McCammon, J. A. Effects of HCM cTnI Mutation R145G on Troponin Structure and Modulation by PKA Phosphorylation Elucidated by Molecular Dynamics Simulations. *Biophys. J.* **2015**, *108* (2), 395–407.

(57) Siddiqui, J. K.; Tikunova, S. B.; Walton, S. D.; Liu, B.; Meyer, M.; de Tombe, P. P.; Neilson, N.; Kekenus-Huskey, P. M.; Salhi, H. E.; et al. Myofilament Calcium Sensitivity: Consequences of the Effective Concentration of Troponin I. *Front. Physiol.* **2016**, *7*, 1–14.

(58) Campbell, S. G.; McCulloch, A. D. Multi-scale Computational Models of Familial Hypertrophic Cardiomyopathy: Genotype to Phenotype. *J. R. Soc., Interface* **2011**, *8* (64), 1550–61.

(59) Campbell, S. G.; Lionetti, F. V.; Campbell, K. S.; McCulloch, A. D. Coupling of Adjacent Tropomyosins Enhances Cross-Bridge-Mediated Cooperative Activation in a Markov Model of the Cardiac Thin Filament. *Biophys. J.* **2010**, *98* (10), 2254–2264.

(60) Cunningham, F.; Amode, M. R.; Barrell, D.; Beal, K.; Billis, K.; Brent, S.; Carvalho-Silva, D.; Clapham, P.; Coates, G.; Fitzgerald, S.; et al. Ensembl 2015. *Nucleic Acids Res.* **2015**, *43* (D1), D662–D669.

(61) Sievers, F.; Higgins, D. G. Clustal Omega, Accurate Alignment of Very Large Numbers of Sequences. In *Multiple Sequence Alignment Methods. Methods in Molecular Biology (Methods and Protocols)*; Russell, D., Ed. Human Press: Totowa, NJ, 2014; Vol. 1079, pp 105–116.

(62) Thompson, J.; Baker, D. Incorporation of Evolutionary information into Rosetta Comparative Modeling. *Proteins: Struct., Funct., Genet.* **2011**, *79* (8), 2380–2388.

(63) Soman, J.; Tao, T.; Phillips, G. N. Conformational Variation of Calcium-bound Troponin C. *Proteins: Struct., Funct., Genet.* **1999**, *37* (4), 510–511.

(64) Kellogg, E. H.; Leaver-Fay, A.; Baker, D. Role of Conformational Sampling in Computing Mutation Induced Changes in Protein Structure and Stability. *Proteins: Struct., Funct., Genet.* **2011**, *79* (3), 830–838.

(65) Pettersen, E. F.; Goddard, T. D.; Huang, C. C.; Couch, G. S.; Greenblatt, D. M.; Meng, E. C.; Ferrin, T. E. UCSF Chimera - A Visualization System for Exploratory Research and Analysis. *J. Comput. Chem.* **2004**, *25* (13), 1605–1612.

(66) Spyropoulos, L.; Li, M. X.; Sia, S. K.; Gagne, S.; Chandra, M.; Solaro, R. J.; Sykes, B. D. Calcium-Induced Structural Transition in the Regulatory Domain of Human Cardiac Troponin C. *Biochemistry* **1997**, *36* (40), 12138–12146.

(67) Phillips, J. C.; Braun, R.; Wang, W.; Gumbart, J.; Tajkhorshid, E.; Villa, E.; Chipot, C.; Skeel, R. D.; Kale, L.; Schulten, K. Scalable Molecular Dynamics with NAMD. *J. Comput. Chem.* **2005**, *26* (16), 1781–1802.

(68) Brooks, B. R.; Brooks, C. L.; Mackerell, A. D.; Nilsson, L.; Petrella, R. J.; Roux, B.; Won, Y.; Archontis, G.; Bartels, C.; Boresch, S.; et al. CHARMM: The Biomolecular Simulation Program. *J. Comput. Chem.* **2009**, *30* (10), 1545–1614.

(69) Fiorin, G.; Klein, M. L.; Hémin, J. Using Collective Variables to Drive Molecular Dynamics Simulations. *Mol. Phys.* **2013**, *111* (22–23), 3345–3362.

(70) Bhandarkar, M.; Bhatele, A.; Bohm, E.; Brunner, R.; Buelens, F.; Chipot, C.; Dalke, A.; Dixit, S.; Fiorin, G.; Freddolino, P. et al. *NAMD User's Guide*, version 2.9; University of Illinois at Urbana-Champaign, Urbana, IL, 2012.

(71) Grossfield, A. WHAM: the Weighted Histogram Analysis Method, version 2.0.9; <http://membrane.urmc.rochester.edu/content/wham> (accessed July 18, 2018).

(72) Hunter, J. D. Matplotlib: A 2D Graphics Environment. *Comput. Sci. Eng.* **2007**, *9* (3), 90–95.

(73) Li, M. X.; Gagne, S. M.; Spyropoulos, L.; Kloks, C. P. A. M.; Audette, G.; Chandra, M.; Solaro, R. J.; Smillie, L. B.; Sykes, B. D. NMR Studies of Ca²⁺ Binding to the Regulatory Domains of Cardiac and E41A Skeletal Muscle Troponin C Reveal the Importance of Site I to Energetics of the Induced Structural Changes. *Biochemistry* **1997**, *36* (41), 12519–12525.

(74) Ohio Supercomputer Center, 1987.